(1992); M. Noble, A. Musacchio, M. Saraste, S. A. Courtneidge, R. Wierenga, *EMBO J.* **12**, 2617 (1993); T. V. Borchert, M. Matthieu, J. P. Zeelen, S. A. Courtneidge, R. Wierenga, *FEBS Lett.* **341**, 79 (1994).
14. J. Janin, S. Miller, C. Chotia, *J. Mol. Biol.* **204**, 155 (1988).
15. M. J. Eck, S. K. Atwell, S. E. Shoelson, S. C. Harrison, *Nature* **368**, 764 (1994).
16. C. H. Lee *et al.*, *Structure* **2**, 423 (1994).
17. G. Waksman *et al.*, *Nature* **358**, 646 (1992); V. Mikol *et al.*, *J. Mol. Biol.* **246**, 344 (1995).
18. D. Cussac, M. Frech, P. Chardin, *EMBO J.* **13**, 4011 (1994).
19. T. A. Jones *et al.*, *Acta Crystallogr.* **D47**, 110 (1991).
20. Collaborative Computational Project, Number 4, *ibid.* **D50**, 760 (1994).
21. A. T. Brünger, *X-PLOR Version 3.1: A system for X-ray Crystallography and NMR* (Yale Univ. Press, New Haven, CT, 1992).
22. P. J. Kraulis, *J. Appl. Crystallogr.* **24**, 946 (1991).
23. E. A. Merritt, M. P. Murphy, *Acta Crystallogr.* **D50**, 869 (1994).
24. We thank F. Schweighoffer for providing the Grb2 gene construct. We are greatly indebted to R. Fourme and J. P. Benoit for development of the DW32 station and to LURE for express runs. We thank P. Saludjian for help in the use of the AMoRe program, M. Eck and S. Harrison for providing Lck coordinates prior to publication, and B. Tocqué and J. Janin for critical reading of the manuscript. S.M. is supported by MESR and BioAvenir. This project was supported by CNRS and was carried out as part of the BioAvenir program supported by Rhône-Poulenc with the participation of Ministere de l'Enseignement Superieur et de la Recherche and the French Ministry of Industry.

27 January 1995; accepted 2 March 1995

Recruitment and Activation of PTP1C in Negative Regulation of Antigen Receptor Signaling by FcγRIIB1

Daniele D'Ambrosio, Keli L. Hippen, Stacey A. Minskoff, Ira Mellman, Giovanni Pani, Kathy A. Siminovitch, John C. Cambier*

Coligation of the Fc receptor on B cells, FcγRIIB1, with the B cell antigen receptor (BCR) leads to abortive BCR signaling. Here it was shown that the FcγRIIB1 recruits the phosphotyrosine phosphatase PTP1C after BCR coligation. This association is mediated by the binding of a 13–amino acid tyrosine-phosphorylated sequence to the carboxyl-terminal Src homology 2 domain of PTP1C and activates PTP1C. Inhibitory signaling and PTP1C recruitment are dependent on the presence of the tyrosine within the 13–amino acid sequence. Inhibitory signaling mediated by FcγRIIB1 is deficient in *motheaten* mice which do not express functional PTP1C. Thus, PTP1C is an effector of BCR-FcγRIIB1 negative signal cooperativity.

For decades it has been known that immune complexes consisting of antigen and immunoglobulin G (IgG) antibodies are potent inhibitors of humoral immune responses (*1*). Immune complex–mediated inhibition of antibody production has been shown to depend on coligation of BCR and the receptor for the Fc region of IgG (FcγRIIB1) and does not result from independent ligation of the FcγRIIB1 (*2*). Studies indicate that FcγRIIB1 coligation aborts the immune response at the level of BCR signal transduction. BCR signal transduction is mediated by the rapid activation of Src and Syk family tyrosine kinases (*3*), augmented protein tyrosine phosphorylation (*4*), phosphoinositide hydrolysis, and elevation of the cytoplasmic free calcium concentration ($[Ca^{2+}]_i$), which result in B cell proliferation, differentiation, and antibody secretion (*5*). Coligation of BCR and FcγRIIB1 leads to the premature termination of inositol trisphosphate (IP_3) production (*6*), inhibition of the extracellular Ca^{2+} influx (*7*), and blockade of blastogenesis (*8*).

FcγRIIB1 is the only receptor for IgG Fc domains that is detectable on the surface of B lymphocytes (*9*). Mutational analysis of this receptor has revealed that a 13–amino acid motif in the cytoplasmic domain is required for negative signaling (*10*). Muta *et al.* showed that this 13–amino acid sequence mediates inhibitory signaling when it is expressed in an inert receptor context, that phosphorylation of Tyr^{309} in this 13–amino acid "inhibitor" sequence follows BCR coligation, and that this tyrosine is essential for FcγRIIB1-mediated inhibitory signaling (*11*). Although this sequence has only been described in a single receptor, it is operationally termed ITIM (immune receptor tyrosine-based inhibitor motif) in this report. It seemed plausible, given the documentation in many systems of protein phosphotyrosine interaction with SH2 domains (*12*), that this inhibitory signaling might be mediated by FcγRIIB1 recruitment of one or more effectors which bind by means of their SH2 domains to the phosphorylated Tyr^{309} in the ITIM.

To identify such a hypothetical effector we used synthetic nonphosphorylated and tyrosine-phosphorylated (designated by the prefix "p") ITIM peptides with the sequence EAENTIT(p)YSLLKH to isolate binding proteins in lysates of [^{35}S]methionine-labeled A20 cells (*13*). Three proteins, of 160, 70, and 65 kD, bound to pITIM but not to nonphosphorylated ITIM (Fig. 1A). These proteins were purified from 5×10^9 A20 cells by pITIM affinity chromatography and subsequent elution with *p*-nitrophenyl phosphate (*p*NPP is a phosphotyrosine analog), followed by SDS–polyacrylamide gel electrophoresis (PAGE) fractionation and membrane transfer as described (*14*), and subjected to sequence analysis. The NH_2-terminal 17–amino acid sequence of the 65-kD protein was found to be a perfect match for the phosphotyrosine phosphatase PTP1C, also known as HCP, SHP, or SH-PTP1 (*15*). We confirmed the identity of the protein by immunoblotting with antibody to PTP1C (anti-PTP1C) (Fig. 1B). Equal amounts of PTP1C were present in pITIM peptide adsorbates of unstimulated A20 cells, A20 cells stimulated with rabbit antibody against membrane immunoglobulin (mIg), and A20 cells stimulated with $F(ab')_2$ fragments of the antibody (Fig. 1B). This suggests that the association of PTP1C with FcγRIIB1 does not require BCR-induced modification of the enzyme.

To address the physiological relevance of the FcγRIIB1-PTP1C interaction, we determined whether this association occurs in cells. Using the monoclonal antibody 2.4G2 we immunoprecipitated FcγRIIB1 from unstimulated A20 cells and from A20 cells that had been stimulated with intact or $F(ab')_2$ rabbit anti-mIg (*16*). Sequential immunoblotting of SDS-PAGE–fractionated material with anti-FcγRIIB, anti-phosphotyrosine, and anti-PTP1C showed inductive FcγRIIB1 tyrosine phosphorylation (Fig. 1C) and PTP1C co-immunoprecipitation (Fig. 1E) only in cells stimulated with intact anti-mIg. Stimulation had no effect on the amount of FcγRIIB1 immunoprecipitated (Fig. 1D). The stimulation with $F(ab')_2$ anti-mIg did not induce FcγRIIB1 tyrosine phosphorylation or PTP1C association (Fig. 1, C and E). In similar experiments performed with IIA1.6 cells [an FcγRIIB1-negative variant of the A20 cell line (*17*)] neither tyrosine-phosphorylated protein nor PTP1C coprecipitation with the 2.4G2 antibody was detected (*18*). These data demonstrate that BCR-FcγRIIB1 coligation is

D. D'Ambrosio, K. L. Hippen, J. C. Cambier, Division of Basic Sciences, Department of Pediatrics, National Jewish Center for Immunology and Respiratory Medicine, 1400 Jackson Street, Denver, CO 80206, and Department of Microbiology and Immunology, University of Colorado Health Science Center, Denver, CO 80206, USA.
S. A. Minskoff and I. Mellman, Department of Cell Biology, Yale University, School of Medicine, New Haven, CT 06520, USA.
G. Pani and K. A. Siminovitch, Samuel Lunenfeld Research Institute of Mount Sinai Hospital, Toronto, Ontario, Canada, M5G1X5.

*To whom correspondence should be addressed.

necessary for FcγRIIB1 tyrosine phosphorylation and association with PTP1C, and therefore suggest that tyrosine phosphorylation of FcγRIIB1 leads to the recruitment of PTP1C to the activated BCR complex.

Having identified the tyrosine-phosphorylated ITIM as the FcγRIIB1 binding site for PTP1C, we next investigated the site within PTP1C which mediates this interaction. PTP1C contains two adjacent SH2 domains (*15*) (herein referred to as NH_2- and COOH-terminal) which could mediate pITIM binding. Association of this phosphatase with tyrosine-phosphorylated c-Kit and with the β chain of the interleukin-3 (IL-3) receptor via the interaction of the NH_2-terminal SH2 domain with phosphotyrosine has recently been reported (*19, 20*). To map the PTP1C binding site for the pITIM, we used glutathione-S-transferase (GST) fusion proteins of the PTP1C SH2 domains expressed together or separately to adsorb lysates of A20 and IIA1.6 cells that were unstimulated or stimulated with intact or $F(ab')_2$ anti-mIg. Immunoblotting with anti-phosphotyrosine revealed that a number of tyrosine-phosphorylated proteins were precipitated (Fig. 2). FcγRIIB1 was precipitated by fusion proteins containing both SH2 domains, or the COOH-terminal but not the NH_2-terminal SH2 only, after BCR-FcγRIIB1 coligation in A20 but not in IIA1.6 cells. Binding studies with pITIM peptide and PTP1C fusion proteins also showed direct binding to the COOH-terminal SH2 domain of PTP1C (*18*).

FcγRIIB1 may mediate inhibitory signaling by modulating PTP1C activity or by translocating active enzyme to the BCR complex, or by both means. Studies of the related phosphatase PTP1D have shown that its activity can be regulated by tyrosine phosphorylation of the enzyme (*21*) as well as by binding of the NH_2-terminal SH2 domain to phosphotyrosine $pTyr^{1009}$ within the platelet-derived growth factor (PDGF) receptor (*22*). Although PTP1C is reportedly tyrosine-phosphorylated as a result of c-Kit ligation, colony-stimulating factor 1 (CSF-1) stimulation, and CD4 or CD8 cross-linking on thymocytes (*19, 23*), we have not detected consistent tyrosine phosphorylation of PTP1C in response to BCR-FcγRIIB1 coligation. To examine the effect of receptor coligation on PTP1C activity, we first assayed the phosphatase activity of PTP1C immunoprecipitated from unstimulated A20 cells and A20 cells stimulated with intact or $F(ab')_2$ anti-mIg. There was no significant modulation of the phosphatase activity upon stimulation. These findings suggested that PTP1C activity may not be regulated by BCR-FcγRIIB1 coligation–dependent signaling. However, it seemed possible that potential regulation resulting from the binding of SH2 to phosphotyrosine might be lost during immunoprecipitation because of complex dissociation (*24*).

The activity of isolated PTP1C was assayed in the presence or absence of pITIM peptide by measuring the release of ^{32}P from the phosphorylated Fyn autophosphorylation site peptide. PTP1C was isolated by pITIM peptide affinity chromatography and elution with *p*NPP. After removing *p*NPP by dialysis, we incubated PTP1C with nonphosphorylated or tyrosine-phosphorylated ITIM or control peptides. The pITIM peptide caused more than a fivefold increase in the specific activity of the enzyme (Fig. 3). The nonphosphorylated ITIM did not affect activity, whereas other tyrosine-phosphorylated peptides [Ig-α and FcεRI-β immune receptor tyrosine-based activation motifs (ITAMs)] significantly inhibited the release of ^{32}P, presumably by means of substrate competition (Fig. 3). The lack of a substrate competition effect by the pITIM peptide is consistent with the finding that this peptide acted as a poor PTP1C substrate in parallel experiments. Thus, the association of PTP1C with the tyrosine-phosphorylated

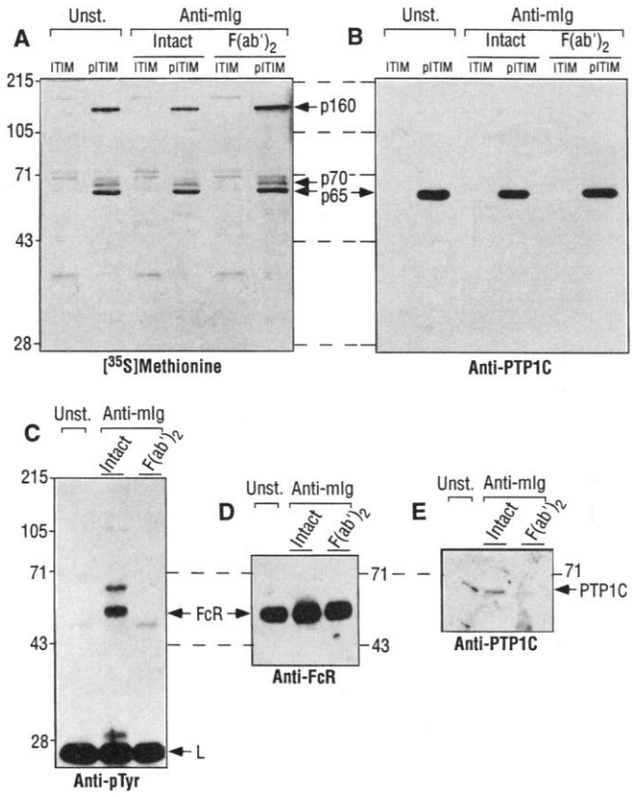

Fig. 1. Association of PTP1C with tyrosine-phosphorylated FcγRIIB1 ITIM. A20 B lymphoma cells were cultured without stimulus (unst.) or stimulated with intact or $F(ab')_2$ rabbit antibody to mIg (anti-mIg). (**A** and **B**) Lysates of [^{35}S]methionine-labeled A20 cells were incubated with nonphosphorylated ITIM and tyrosine-phosphorylated pITIM peptide. (**C** to **E**) FcγRIIB1 (FcR) was immunoprecipitated from A20 cell lysates. The peptide adsorbates were eluted with SDS reducing sample buffer, fractionated by SDS-PAGE, and transferred to Immobilon-P membranes, and then the membranes were subjected to autoradiography (A) or immunoblotting with anti-PTP1C (B). Immunoprecipitates were eluted with formic acid and similarly fractionated and transferred to membranes that were subjected to sequential immunoblotting with anti-phosphotyrosine (anti-pTyr) (C), anti-FcγRIIB (D), and anti-PTP1C (E) (*14*). Arrows indicate the positions of pITIM peptide–adsorbed proteins of 160, 70, and 65 kD in (A), and the positions of FcγRIIB1, PTP1C, and the light chain (L) of the precipitating antibody in (C) to (E). Positions of molecular size markers are indicated to the left in kilodaltons.

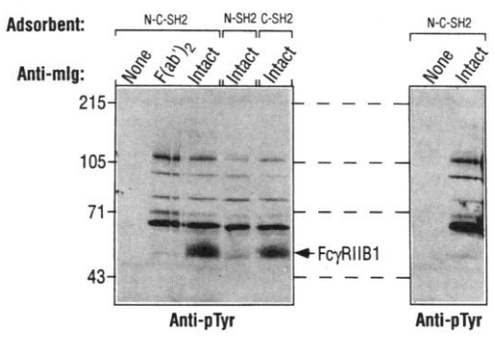

Fig. 2. Interaction of PTP1C with tyrosine-phosphorylated FcγRIIB1 is mediated by the COOH-terminal SH2 domain of PTP1C. Glutathione Sepharose–bound GST fusion proteins containing the PTP1C NH_2- and COOH-terminals (N-SH2 C-SH2) or only the NH_2- or the COOH-terminal SH2 domains (N-C-SH2) were used to adsorb detergent lysates of A20 cells that had been cultured without stimulus or stimulated with intact or $F(ab')_2$ anti-mIg (left panel). Alternatively, the tandem SH2 domain fusion protein was used to adsorb lysates of IIA1.6 cells which had been cultured without stimulus or stimulated with intact anti-mIg (right panel) (*27*). All adsorbates were fractionated by SDS-PAGE and transferred to Immobilon-P membranes which were subjected to anti-phosphotyrosine (anti-pTyr) immunoblotting. The arrow indicates the position of FcγRIIB1. Positions of molecular size markers are indicated to the left in kilodaltons.

FcγRIIB1 is potentially important not only for recruitment of the phosphatase to the FcγRIIB1, but also for regulation of its activity.

It has been reported that phosphorylation of the tyrosine in the ITIM is required for FcγRIIB1 inhibitory signaling (*11*), which would be consistent with an essential role for PTP1C in this function. To extend this correlation, we investigated the binding of PTP1C to a mutated FcγRIIB1 which lacks the ITIM tyrosine. Truncated FcγRIIB1 receptors retaining the wild-type ITIM (CT314 WT) or with a tyrosine-to-alanine (Y→A) substitution in the ITIM (CT314 Y309A) were expressed in IIA1.6 cells (Fig. 4, A to C), and tyrosine phosphorylation, PTP1C binding, and the ability of these transfected receptors to inhibit Ca^{2+} mobilization after coligation with the BCR was assessed. Stimulation with $F(ab')_2$ anti-mIg of IIA1.6 cells expressing the CT314 WT induced a prolonged increase of $[Ca^{2+}]_i$, which was significantly reduced in duration when stimulation was performed with intact anti-mIg (Fig. 4, D and E). These results indicated that the truncation does not significantly impair the previously described FcγRIIB1 inhibition of extracellular Ca^{2+} influx (*7*). This Fc receptor was tyrosine-phosphorylated (Fig. 4F, panel a) and bound PTP1C (Fig 4F, panel c). In contrast, IIA1.6 cells expressing CT314 Y309A showed similar late phase Ca^{2+} mobilization after stimulation with intact or $F(ab')_2$ anti-mIg (Fig. 4, D and E), indicating that the tyrosine of the ITIM is essential for complete inhibition of Ca^{2+} mobilization. However, a modest inhibition of Ca^{2+} mobilization was still detectable in response to BCR coligation with the CT314 Y309A mutant (Fig. 4E), suggesting that other regions within the cytoplasmic domain may play a role in FcγRIIB1-mediated negative signaling. Alternatively, the nonphosphorylatable ITIM may still interact to some degree with PTP1C or other effectors. The CT314 Y309A receptor was not phosphorylated and did not bind PTP1C after BCR coligation (Fig. 4G). These data indicate that tyrosine phosphorylation of the ITIM is important for PTP1C association as well as FcγRIIB1-mediated negative signaling, suggesting that PTP1C action is necessary for FcγRIIB1 function. However, on the basis of the data presented above, it is still possible that the requirement for Tyr^{309} may reflect a need to interact with some other pITIM binding proteins, for example, the 160- or 70-kD proteins. This question can only be addressed by analysis of FcγRIIB1 function in a PTP1C-negative cellular context.

A complete or partial lack of expression of PTP1C has been reported in the *motheaten* (*me/me*) and the *motheaten viable* (me^v/me^v) mouse, respectively, where it appears to constitute the molecular basis of the immune system dysregulation (*25*). The mechanism by which the lack of PTP1C causes aberrant immune function in the *motheaten* mouse is obscure, but studies described here suggest that a deficiency of

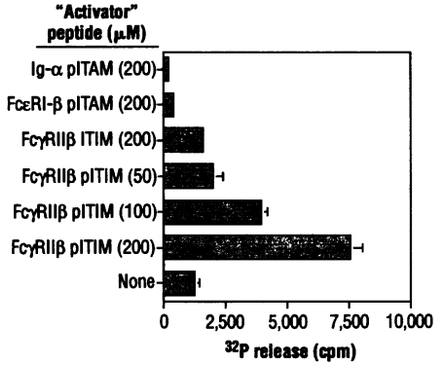

Fig. 3. Up-regulation of PTP1C activity by the tyrosine-phosphorylated FcγRIIB1 ITIM. Sepharose beads conjugated to synthetic tyrosine-phosphorylated pITIM peptide were used to adsorb lysates of A20 cells. The pITIM-bound PTP1C was eluted with *p*NPP in phosphatase buffer, and *p*NPP was removed by dialysis. The Fyn autophosphorylation site peptide [RRLIEDNE(p)YTARQGA] was used as the substrate in the phosphatase assay. The release of ^{32}P from the substrate was determined (*29*) in the absence or presence of various amounts of nonphosphorylated or tyrosine-phosphorylated FcγRIIB ITIM peptide, or tyrosine-phosphorylated Ig-α and FcεRI-β ITAM peptide (*28*), respectively, with the amino acid sequences ENL(p)YEGLNLDDCSM(p)YEDI and DRL(p)YEELNHV(p)YSPI(p)YSEL. The data are representative of three independent experiments performed in duplicate. The bars reflect the range of the values obtained in a representative experiment.

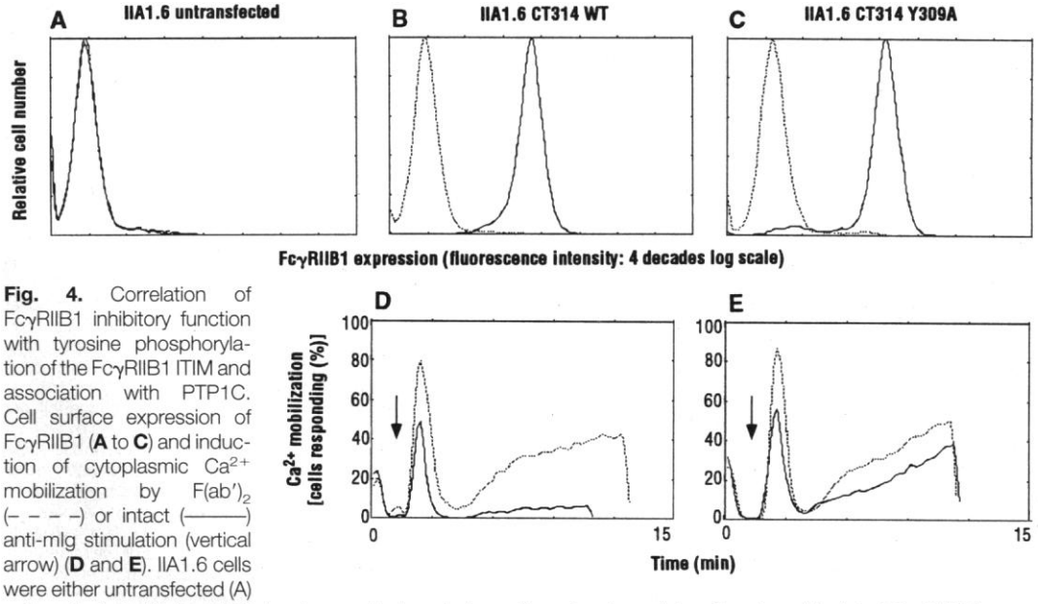

Fig. 4. Correlation of FcγRIIB1 inhibitory function with tyrosine phosphorylation of the FcγRIIB1 ITIM and association with PTP1C. Cell surface expression of FcγRIIB1 (**A** to **C**) and induction of cytoplasmic Ca^{2+} mobilization by $F(ab')_2$ (– – – –) or intact (———) anti-mIg stimulation (vertical arrow) (**D** and **E**). IIA1.6 cells were either untransfected (A) or transfected with FcγRIIB1 bearing a cytoplasmic truncation at amino acid residue 314 (CT314 WT) (B and D) or transfected with FcγRIIB1 bearing a cytoplasmic truncation at amino acid residue 314 and in which the Tyr^{309} of the ITIM was substituted with alanine (CT314 Y309A) (C and E) (*30*). CT314 WT (**F**) and CT314 Y309A (**G**) FcγRIIB1 were immunoprecipitated from IIA1.6-transfected cells unstimulated (Unst.) or stimulated with intact or $F(ab')_2$ anti-mIg.

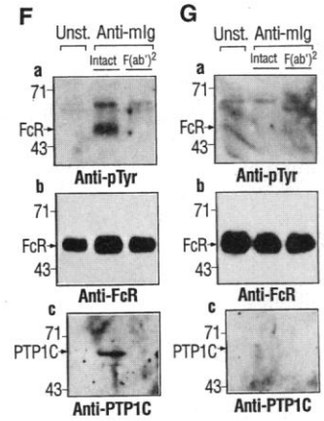

Formic acid–eluted FcγRIIB1 immunoprecipitates were fractionated by SDS-PAGE and transferred to Immobilon-P membranes which were then subjected to immunoblotting with anti-phosphotyrosine (anti-pTyr) (panel a), anti-FcγRIIB1 (anti-FcR) (panel b), and anti-PTP1C (panel c) as described for Fig. 1. The positions of FcγRIIB1 and PTP1C are indicated by arrows. The positions of molecular size markers were indicated to the left in kilodaltons.

PTP1C could exert its effects by impairing FcγRIIB1-mediated negative regulation of B cell function. The hyperimmunoglobulinemia and production of multiple autoantibodies reported in the *motheaten* mouse suggest that the immune system fails to control B cell activation (*26*), which is consistent with a deficit in negative regulation via FcγRIIB1.

To analyze the function of FcγRIIB1 in the *motheaten* mouse, we isolated splenic B cells and measured Ca^{2+} mobilization in response to BCR ligation or BCR-FcγRIIB1 coligation. These experiments revealed that B cells from *motheaten* mice were greatly hyporesponsive even to $F(ab')_2$-mediated BCR ligation when compared with age-matched normal littermates. The coligation of FcγRIIB1 resulted in a diminished Ca^{2+} mobilization in the normal but not in the *motheaten* mouse B cells, consistent with our hypothesis. However, the interpretation of these experiments was difficult because of the reduced Ca^{2+} mobilization in response to all stimuli seen in the *motheaten* mouse B cells. As an alternative approach to analyzing the role of PTP1C in FcγRIIB1 function, we compared the proliferative responses of normal and *motheaten* mouse B cells to $F(ab')_2$ and intact anti–mouse Ig. Whereas normal B cells (48 hours after optimal stimulation) exhibited a much reduced response to intact antibodies (300 cpm) compared with $F(ab')_2$ antibodies (3700 cpm), *motheaten* B cells (*me/me*) responded equivalently to intact antibodies (3000 cpm) and $F(ab')_2$ (2700 cpm). B cells from *motheaten viable* mice (me^v/me^v) showed a partial responsiveness to intact antibodies (3800 cpm) when compared with $F(ab')_2$ (4900 cpm). These data confirm that PTP1C is necessary for FcγRIIB1 inhibition of BCR signal transduction.

Signaling by the FcγRIIB1 is likely to be involved in the regulation of antibody production during the course of the immune response by virtue of immune complex–mediated BCR-FcγRIIB1 coligation. Our studies identify the phosphotyrosine phosphatase PTP1C as a mediator of FcγRIIB1 function. PTP1C appears to be recruited and activated by means of COOH-terminal SH2 domain–mediated binding to the tyrosine-phosphorylated FcγRIIB1 ITIM. Our results also suggest that the immune dysfunction reported in the PTP1C-deficient *motheaten* mouse is, at least in part, the result of impaired FcγRIIB1 function. The mechanism of action of PTP1C and its complex role in the regulation of immune functions are only beginning to yield to investigation. Further studies will be required for identification of the substrates of PTP1C and to address the specific role of this enzyme in regulation of the immune response.

REFERENCES AND NOTES

1. P. L. Chan and N. R. S. C. Sinclair, *Immunology* **21**, 967 (1971); H. Kohler, B. C. Richardson, D. A. Rowley, S. Danyk, *J. Immunol.* **119**, 1979 (1977).
2. N. E. Phillips and D. C. Parker, *J. Immunol.* **130**, 602 (1983).
3. A. L. Burkhardt, M. Brunswick, J. B. Bolen, J. J. Mond, *Proc. Natl. Acad. Sci. U.S.A.* **88**, 7410 (1991); T. Yamada *et al.*, *Eur. J. Biochem.* **213**, 455 (1993).
4. M. R. Gold, D. A. Law, A. L. DeFranco, *Nature* **345**, 810 (1990).
5. J. C. Cambier and J. T. Ransom, *Annu. Rev. Immunol.* **5**, 175 (1987); C. M. Pleiman, D. D'Ambrosio, J. C. Cambier, *Immunol. Today* **15**, 393 (1994).
6. J. Bijsterbosch and G. G. B. Klaus, *J. Exp. Med.* **162**, 1825 (1985).
7. D. Choquet *et al.*, *J. Cell. Biol.* **121**, 355 (1993); H. A. Wilson *et al.*, *J. Immunol.* **138**, 1712 (1987).
8. N. E. Phillips and D. C. Parker, *J. Immunol.* **132**, 627 (1984).
9. J. C. Unkeless, E. Scigliano, V. H. Freedman, *Annu. Rev. Immunol.* **6**, 251 (1988).
10. S. Amigorena *et al.*, *Science* **256**, 1808 (1992); W. H. Fridman *et al.*, *Immunol. Rev.* **125**, 49 (1992).
11. T. Muta *et al.*, *Nature* **368**, 70 (1994).
12. L. C. Cantley *et al.*, *Cell* **64**, 281 (1991); C. A. Koch, D. Anderson, M. F. Moran, C. Ellis, T. Pawson, *Science* **252**, 668 (1991).
13. K. J. Kim, C. Kanellopoulos-Langevin, R. M. Merwin, D. H. Sachs, A. Aofsky, *J. Immunol.* **122**, 549 (1979). Abbreviations for the amino acid residues are as follows: A, Ala; C, Cys; D, Asp; E, Glu; F, Phe; G, Gly; H, His; I, Ile; K, Lys; L, Leu; M, Met; N, Asn; P, Pro; Q, Gln; R, Arg; S, Ser; T, Thr; V, Val; W, Trp; and Y, Tyr.
14. Cells (10^8/ml) were stimulated for 2 min at 37°C with $F(ab')_2$ (12 μg/ml) or intact (20 μg/ml) anti-mIg. Unstimulated and stimulated cells were lysed in 1% NP-40 lysis buffer [1% NP-40, 150 mM NaCl, 10 mM tris-HCl (pH 7.4), 2.0 mM sodium orthovanadate, 10 mM sodium pyrophosphate, 0.4 mM EDTA, 10 mM NaF, 1 mM phenylmethylsulfonyl fluoride, and 2 μg/ml each of aprotinin, leupeptin, and α-1-antitrypsin] and spun 5 min at 14,000 rpm in an Eppendorf microfuge to remove detergent-insoluble material. FcγRIIB1 was immunoprecipitated from cleared lysates (5×10^7 cell equivalents) with 2.4G2 monoclonal antibody (*16*) conjugated to Sepharose beads (30 μg per 25 μl of a 50% slurry) for 15 min at 4°C. Cleared lysates (2×10^7 cell equivalents) were also adsorbed with peptide-coupled Sepharose beads (20 μg per 10 μl of a 50% slurry) for 1 hour at 4°C. Immunoprecipitates and peptide adsorbates were then washed three times in lysis buffer. The immunoprecipitated material was eluted with 2.2% formic acid (0.1 ml), lyophilized, and resuspended in SDS reducing sample buffer (0.1 ml). Peptide adsorbates were directly eluted with SDS reducing sample buffer (0.1 ml). Eluted immunoprecipitates and peptide adsorbates were then fractionated by 10% SDS-PAGE and transferred electrophoretically to Immobilin-P membranes (Millipore). Membranes were blocked with 5% bovine serum albumin (BSA) in tris-buffered saline (TBS). Immunoblots were developed with an enhanced chemiluminescence (ECL) detection system (Amersham) after incubation with horseradish peroxidase–conjugated protein A for anti-PTP1C, goat antibody to mouse Ig for anti-phosphotyrosine, and goat antibody to rat Ig for FcγRIIB1. Anti-PTP1C was obtained by immunizing rabbits with the NH_2-terminal portion of PTP1C cleaved from a bacterially expressed GST fusion protein (amino acid residues 1 to 193).
15. S.-H. Shen, L. Bastien, B. I. Posner, P. Chretien, *Nature* **352**, 736 (1991); R. J. Matthews, D. B. Bowne, E. Flores, M. L. Thomas, *Mol. Cell. Biol.* **12**, 2396 (1992); J. Plutzky, B. G. Neel, R. D. Rosemberg, *Proc. Natl. Acad. Sci. U.S.A.* **89**, 1123 (1992).
16. J. C. Unkeless, *J. Exp. Med.* **150**, 580 (1979).
17. B. Jones, J. P. Tite, C. A. Janeway, *J. Immunol.* **136**, 348 (1986).
18. D. D'Ambrosio and J. C. Cambier, unpublished results.
19. T. Yi and J. Ihle, *Mol. Cell. Biol.* **13**, 3350 (1993).
20. T. Yi, A. L.-F. Mui, G. Krystal, J. N. Ihle, *ibid.*, p. 7577.
21. W. Vogel, R. Lammers, J. Huang, A. Ullrich, *Science* **259**, 1611 (1993).
22. R. J. Lechleider *et al.*, *J. Biol. Chem.* **268**, 21478 (1993).
23. Y. G. Yeung, K. L. Berg, F. J. Pixley, R. H. Angeletti, E. R. Stanley, *ibid.* **267**, 23447 (1992); U. Lorenz *et al.*, *Mol. Cell. Biol.* **14**, 1824 (1994).
24. S. Felder *et al.*, *Mol. Cell. Biol.* **13**, 1449 (1993); G. Panayotou *et al.*, *ibid.*, p. 3567.
25. M. Kozlowski *et al.*, *J. Exp. Med.* **178**, 2157 (1993); L. D. Shultz *et al.*, *Cell* **73**, 1445 (1993).
26. M. C. Green and L. D. Shultz, *J. Hered.* **66**, 250 (1975); L. D. Shultz and M. C. Green, *J. Immunol.* **116**, 936 (1976); L. D. Shultz, D. R. Coman, C. L. Bailey, W. G. Beamer, C. L. Sidman, *Am. J. Pathol.* **116**, 179 (1984); L. D. Shultz, *Curr. Top. Microbiol. Immunol.* **137**, 216 (1988).
27. A20 and IIA1.6 cells (10^8/ml) were left unstimulated or stimulated for 2 min at 37°C with intact (50 μg/ml) or $F(ab')_2$ (32 μg/ml) anti-mIg and subsequently lysed in 1% NP-40 lysis buffer, then spun 5 min at 14,000 rpm in an Eppendorf microfuge. Cleared cell lysates (4×10^7 cell equivalents) were adsorbed for 1 hour at 4°C with GST fusion proteins containing PTP1C NH_2- or COOH-terminal or both SH2 domains adsorbed to glutathione Sepharose beads (20 μg per 20 μl of a 50% slurry each) (Pharmacia). After washing the adsorbates three times with lysis buffer, they were eluted with SDS reducing sample buffer (0.1 ml), fractionated by 10% SDS-PAGE, and transferred to Immobilin-P membranes and the membranes subjected to anti-phosphotyrosine immunoblotting as before.
28. This sequence previously termed ARH1, TAM, or ARAM is by consensus renamed ITAM for immune receptor tyrosine-based activation motif [J. C. Cambier, *Immunol. Today* **16**, 110 (1995)].
29. A20 cells (2×10^8) were lysed in 1% NP-40 lysis buffer lacking sodium orthovanadate and sodium pyrophosphate. Cleared lysate (1 ml) was incubated for 1 hour at 4°C with peptide-conjugated beads (250 μg per 100 μl of a 50% slurry). The adsorbate was then washed twice in lysis buffer and once in phosphate buffer [10 mM imidazole (pH 7.0), 50 mM EDTA, 0.1% 2-mercaptoethanol, and BSA (1 mg/ml)]. Bound PTP1C was eluted by incubation for 15 min on ice with 50 mM *p*NPP. The *p*NPP was subsequently removed by centrifugation at 10,000 rpm for 20 min in Centricon 10 (Amicon), and the eluted PTP1C was resuspended in phosphatase buffer (500 μl). The phosphatase assay was performed at 30°C for 15 min in the presence of 20 μl of the eluted PTP1C and 30,000 cpm of the substrate Fyn autophosphorylation site peptide (2 μM) phosphorylated with the B subunit of the insulin receptor kinase in a final volume of 40 μl. The released ^{32}P was separated from the labeled peptide substrate by organic extraction and quantitated as described [K. H. Hippen *et al.*, *Biochemistry* **32**, 12405 (1993)].
30. The complementary DNA (cDNA) encoding FcγRIIB1 was obtained from M. Hogarth (Parkville, Victoria, Australia) and J. Ravetch (New York). Mutants of FcγRIIB1 were generated by polymerase chain reaction, and the sequence of all primers are available on request. The sequences of the cloned fragments were confirmed by dideoxy sequencing, and cDNAs encoding Fc receptors were cloned into the cytomegalovirus-based expression plasmid pCB6. Cells were transfected by electroporation, selected for growth in G418 (0.5 mg/ml), and enriched for high FcγRIIB1 expression by adsorption to bacteriological plates coated with IgG. Cell surface expression of FcγRIIB1 was detected by staining cells with biotinylated 2.4G2 antibody and fluoresceinated avidin (Tago) or with fluoresceinated avidin only and analysis by flow cytometry (FACScan, Becton Dickinson). For measurements of cytoplasmic Ca^{2+} mobilization, 1×10^6 cells were loaded with Indo-1 AM (Molecular Probes) and subsequently stimulated with either $F(ab')_2$ (12 μg/ml) or intact (20 μg/ml) anti-mIg, and $[Ca^{2+}]_i$ was monitored with a flow cytometer for 15 min (model 50H, Ortho Diagnostic Systems) [L. B. Justement, J. Krieger, J. C. Cambier, *J. Immunol.* **143**, 881 (1989)]. The percent of cells that responded was evaluated with an appended data acquisition system and the

MultiTIME software (Phoenix Flow Systems).
31. Supported by grants from the USPHS. D.D. and K.L.H. contributed equally to this work. D.D. is supported by a fellowship from the Associazione Italiana per la Ricerca sul Cancro (AIRC). S.A.M. is an American Cancer Society fellow. J.C.C. is an Ida and Cecil Green Professor of Cell Biology. We thank W. Jensen and C. Pleiman for helpful advice and comments, and J. Franconi for secretarial assistance.

6 December 1994; accepted 15 February 1995

Activity-Dependent Action Potential Invasion and Calcium Influx into Hippocampal CA1 Dendrites

Nelson Spruston,* Yitzhak Schiller, Greg Stuart, Bert Sakmann

The temporal and spatial profile of activity-evoked changes in membrane potential and intracellular calcium concentration in the dendrites of hippocampal CA1 pyramidal neurons was examined with simultaneous somatic and dendritic patch-pipette recording and calcium imaging experiments. Action potentials are initiated close to the soma of these neurons and backpropagate into the dendrites in an activity-dependent manner; those occurring early in a train propagate actively, whereas those occurring later fail to actively invade the distal dendrites. Consistent with this finding, dendritic calcium transients evoked by single action potentials do not significantly attenuate with distance from the soma, whereas those evoked by trains attenuate substantially. Failure of action potential propagation into the distal dendrites often occurs at branch points. Consequently, neighboring regions of the dendritic tree can experience different voltage and calcium signals during repetitive action potential firing. The influence of backpropagating action potentials on synaptic integration and plasticity will therefore depend on both the extent of dendritic branching and the pattern of neuronal activity.

The prevailing view of how neurons function in the central nervous system is that synaptic potentials propagate passively to the soma, where they summate and, if the resulting depolarization is large enough, an action potential is initiated in the axon (*1–5*). In hippocampal CA1 pyramidal neurons, however, evidence exists both for somatic (*3*) and dendritic action potential initiation (*6, 7*). Once initiated, the extent to which action potentials depolarize the dendritic tree could influence neuronal function in a number of ways—for example, by summating with excitatory postsynaptic potentials (EPSPs) or by shunting the dendritic membrane. In CA1 pyramidal neurons, action potential–mediated depolarization can also result in the elevation of dendritic intracellular calcium concentration ($[Ca^{2+}]_i$) (*8, 9*), which is important for the induction of long-term changes in synaptic strength (*10–12*).

Simultaneous somatic and dendritic recordings (*13*) revealed that both the inflection point and the peak of action potentials evoked by threshold synaptic stimulation (Fig. 1A) or somatic or dendritic current pulses always occurred first at the soma (Fig. 1B). Similar results were observed for synaptically evoked action potentials recorded extracellularly in cell-attached patches (*14*). In a few cases, however, when synaptic stimulus intensities several times the threshold value were used, the site of action potential initiation shifted into the proximal dendrites. Therefore the usual site of tetrodotoxin (TTX)-sensitive action potential initiation in CA1 pyramidal neurons is near the soma (presumably in the axon) (*3*), but may shift into the proximal dendrites under some conditions (*15*). Such a shift may explain some previous reports of dendritic action potential initiation (*6*), but it is unclear whether such large, synchronous synaptic activation normally occurs in vivo.

The average conduction velocity of action potentials propagating from the soma back into the proximal 260 μm of the apical dendrites was 0.24 m/s (Fig. 1B). In the most distal simultaneous recordings (~300 μm from the soma), a longer latency was usually observed than would be expected from linear extrapolation of the closer points. This was due to a second inflection on the rising phase of the dendritic action potentials (Fig. 1B, inset). Action potentials in axons have a similar form when propagating close to threshold for failure of active propagation (*16*).

The amplitude of single action potentials measured with dendritic recordings at

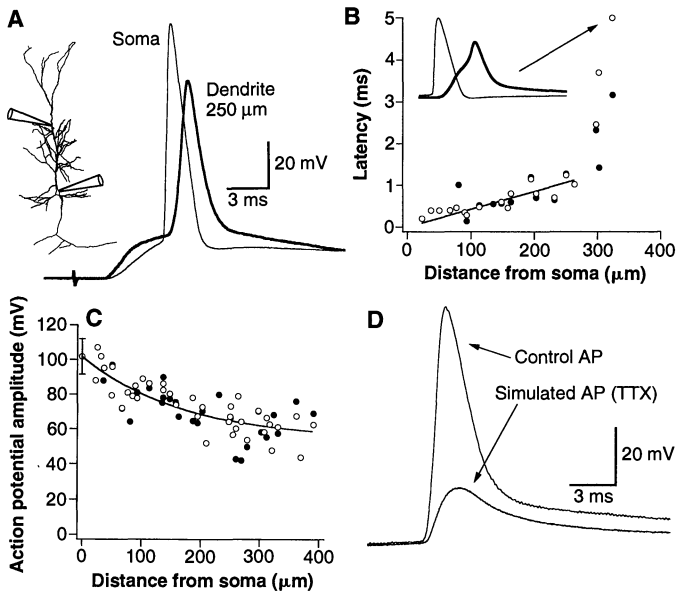

Fig. 1. Action potentials are initiated near the soma and actively invade the dendrites of CA1 pyramidal neurons. (**A**) Action potentials recorded simultaneously from the soma (thinner line) and apical dendrite (thicker line) in response to synaptic stimulation. Note that the action potential occurs first in the somatic recording. The inset shows a camera lucida drawing of the neuron from which the recording was made at the locations indicated (lower pipette, soma). (**B**) Plot of the latency from the peak of the somatic action potential to the peak of the dendritic action potential as a function of distance of the recording site from the soma for all double recordings. Action potentials were evoked either by synaptic stimulation (filled circles) or current pulses (open circles). The straight line is a linear regression fit (forced to pass through the origin) to all points up to 264 μm from the soma, which indicates to a conduction velocity of 0.24 m/s. The inset (105 mV, 20 ms) shows the data for the indicated point. (**C**) Plot of spike amplitude (measured from the inflection point to the peak) as a function of distance of the recording site from the soma for action potentials evoked by either synaptic stimulation (filled circles) or dendritic current pulses (open circles). The somatic action potential amplitude is indicated by a single point (mean ± SD, $n = 30$). The smooth line is an exponential fit to the data (somatic point weighted accordingly) with a distance constant of 170 μm. (**D**) Comparison of the amplitude of a simulated action potential (in the presence of 1 μM TTX) and a control action potential measured at the same dendritic location (210 μm). The simulated action potential was produced by using the action potential measured at the soma as a voltage-clamp command during somatic whole-cell voltage clamp (*13*).

Max-Planck-Institut für medizinische Forschung, Abteilung Zellphysiologie, Jahnstrasse 29, 69120 Heidelberg, Germany.

*To whom correspondence should be addressed.